

It is obvious by the facts that the treatment of the original particles of type I changes the particle shape to the one of type II, and that the crystal structure change also takes place as the x-ray diffraction pattern changes from type α to type β . The purification by dispersing the conc. H_2SO_4 solution into water reverses the above mentioned course, and this cycle can be repeated.

The spacings of lattice planes calculated from the x-ray diffraction patterns are compared in Fig. 4, where Robertson's data are also shown for comparison (Robertson,

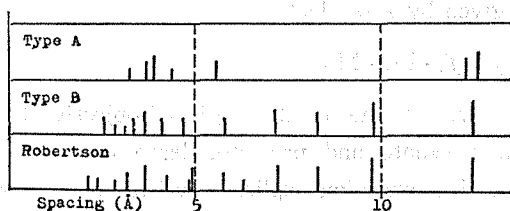


Fig. 4. Spacings of lattice planes of Cu-phthalocyanine.

J. M.: *J. Chem. Soc.*, (1937) 219). It is clear from this that the type β corresponds to the one reported by Robertson, which belongs to the space group $P_{21/a}$. It is suitable to decide that the direction of the crystal growth can be attributed to b -axis and the flaky surface observable in the electron image to (20T) plane from the correspondence to Robertson's data.

9. On the Characteristic Properties of the Three-Stage Electron Microscope SM-C3 as an Electron Diffraction Camera

Eiji SUITO and Natsu UYEDA

(Suito Laboratory)

The consolidated two-stage electron microscope SM-C2 was reconstructed as a three-stage electron microscope, with a projector lens newly added at the rear of the older lens system, electron diffraction chamber, and several movable apertures. This may be called the SM-C3 hereafter, and can be used as the instrument for:

1. Electron microscope having the order of final magnification continuously variable within the range from $500\times$ to $12,000\times$.
2. Dark field electron microscope with the movable objective aperture.
3. Electron micro-diffraction camera for the selected and limited area of the intermediate image of the specimen.
4. Electron shadow microscope.
5. High resolution electron diffraction camera with variable camera length, which can be also fixed if needed.

The stability of the final camera length for selective micro-diffraction method was also investigated under various conditions of the beam potential (V) and exciting current (i) for magnetic lenses. When both of the objective and projector lenses, which have the same number of coil turning (n) are excited under series combination by a common direct current supplied from a power source, the parameter k , which represents the quantity: $0.8 ni/\sqrt{V}$, takes the same value for both of the two lenses, under various values of V and i . The final camera length, L_f , when used as a micro-diffraction camera, is given by a product:

$$L_f = f_0 \cdot M_I \cdot M_P \quad (1)$$

where f_0 , M_I and M_P represent the focal length of objective lens, the order of the magnification of the intermediate and projector lens respectively. When they are substituted by the respective expression explicitly written by the parameter k , the Eq. (1) becomes as follows:

$$L_f = \frac{f_0}{f_p} \left(\frac{l_2 l_3}{l_1} - \frac{l_3}{l_1} f_p \right) = \frac{1}{\sqrt{k^2+1}} \frac{\sin(\pi\sqrt{k^2+1})}{\sin(\pi/\sqrt{k^2+1})} \left(\frac{l_2 l_3}{l_1} - \frac{l_3}{l_1} \cdot f_p \right) \quad (2)$$

where l_1 , l_2 and l_3 are distances between the two neighbouring items among those as objective, intermediate, projector lens and final screen (or photo plate). With practical values of l_1 , l_2 , and l_3 , the value of L_f were calculated by Eq. (2) for various values of i with a fixed beam potential ($V=50$ KV) and plotted as shown in Fig. 1. The

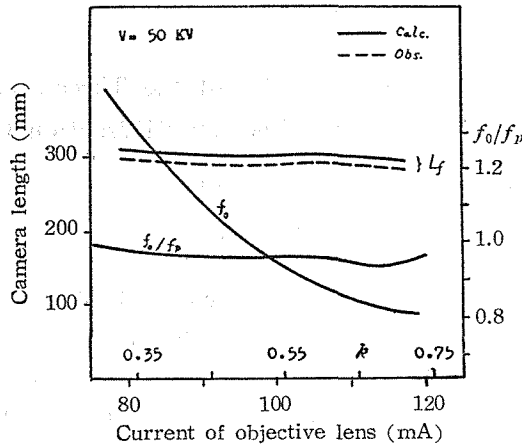


Fig. 1. $L_f \sim i$ relation.

values of L_f has a close relation to the quotient f_0/f_p , therefore this is also plotted against i in Fig. 1. The increase of i decreases sharply the value of f_0 , but the focal length f_p of the projector lens also decreases as i increases, then the quotient f_0/f_p stand almost independent of the variation in i . The variation of L_f also stand almost independent of the variation of the exciting current, though a slight decreasing tendency with increasing value are left over. But it is obvious that this tendency is

very slack in comparison with the case where the focal length of the projector lens is fixed. The experimental values of L_f prove well these relations, and the accordance between the two curves for L_f is very good as shown in Fig. 1.

The L_f - k relation is also investigated under a condition of fixed exciting current i and varying the beam potential (V). The change of L_f against the beam potential V as shown in Fig. 2. The accordance between the calculated and observed values is pretty well, and it is obvious from the results that the camera length L_f has a slight increasing tendency as the beam potential increases.

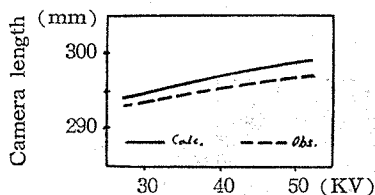


Fig. 2. L_f -V relation.

In both cases, the stability of the camera length for the electron diffraction is rather well, when a three-stage electron microscope is used as an electron micro-diffraction camera.

The rotation angle (φ) in the direction of orientation caused by the intermediate lens, between the electron image and its diffraction pattern is also investigated, and it satisfies the following relation

$$\varphi = \pi k' i n / \sqrt{V} \quad (3)$$

where k' is rather 0.6 than 0.8 as a weak lens with a pole piece of large diameter and gap separation is used for intermediate lens. Practically, it is suitable for estimating the rotation angle to be 1° as the exciting current i of the intermediate lens varies by 1 mA, when the number of coil turning n is about 21,000.

10. The Electron Microscopic and Micro-diffraction Studies of the Changes in Specimens

Nobuji SASAKI and Ryuzo UEDA

(Sasaki Laboratory)

A continual observation of the progress of change of a solid substance undergoing during a physical or chemical treatment by means of the electron microscopy accompanied by the electron diffraction method would provide valuable informations for the clarification of the nature of the process.